



Mathematical Analysis of Two Strains Covid-19 Disease Using SEIR Model

Adetayo Samuel Eegunjobi^{1,*} & Oluwole Daniel Makinde²

¹Mathematics Department, Namibia University of Science and Technology, Windhoek, Namibia

²Faculty of Military Science, Stellenbosch University, Private Bag X2, Saldanha 7395, South Africa

*E-mail: samdet1@yahoo.com

Abstract. The biggest public health problem facing the whole world today is the COVID-19 pandemic. From the time COVID-19 came into the limelight, people have been losing their loved ones and relatives as a direct result of this disease. Here, we present a six-compartment epidemiological model that is deterministic in nature for the emergence and spread of two strains of the COVID-19 disease in a given community, with quarantine and recovery due to treatment. Employing the stability theory of differential equations, the model was qualitatively analyzed. We derived the basic reproduction number R_0 for both strains and investigated the sensitivity index of the parameters. In addition to this, we probed the global stability of the disease-free equilibrium. The disease-free equilibrium was revealed to be globally stable, provided $R_0 < 1$ and the model exhibited forward bifurcation. A numerical simulation was performed, and pertinent results are displayed graphically and discussed.

Keywords: Covid-19 Dynamics; Mathematical Analysis; Reproduction Number; Stability Theory; Two Strains.

1 Introduction

Coronavirus 2019 (COVID-19) is a highly infectious disease caused by a virus. It has been circulating globally and has caused many people to lose their loved ones and relatives. The pandemic started in December 2019 in Wuhan, China and the disease was spread by people travelling for new year inside China [1]. The virus circulates during singing, coughing, sneezing, speaking, or breathing and the particles range from larger respiratory droplets to smaller aerosols [2].

Epidemiology modeling plays a critical role in early warning systems and the avoidance of outbreaks. Nonlinear differential equations are an important tool to illustrate the dynamics of infectious diseases and to evaluate control schemes to stop them. Different mathematical models have been formulated to investigate COVID-19 in various ways. Wickramaarachchi *et al.* [3] adopted an SEIR (susceptible, exposed, infected, and recovered) type mathematical model to

Received November 7th, 2021, Revised May 21st, 2022, Accepted for publication November 4th, 2022

Copyright © 2022 Published by ITB Institut for Research and Community Service, ISSN: 2337-5760,

DOI: 10.5614/j.math.fund.sci.2022.54.2.1

outline the dynamics of COVID-19 in Sri Lanka. They focused on examining the monitoring measures against the disease's transmission and the time of implementation in the community during the epidemic's initial months. Their analysis concluded that if policymakers put up strict control measures, peaks can be delayed, and the curve can be flattened. Moshen [4] probed the global stability of a COVID-19 model with a quarantine approach together with the effect of media coverage. This may have been as a result of fear the media was spreading about the disease's reproduction number. From their analysis, they surmised that the reproduction number clearly conformed to the disease's transmission rate. Seidu [5] developed and analyzed a deterministic ordinary differential equation model for SARS-CoV-2 in view of the function of exposed, mildly symptomatic, and severe symptomatic cases in terms of the disease's transmission. Their analysis revealed that reduction of contact via the use of nasal masks and physical distancing reduces SARS-CoV-2 transmission. Alshammari [6] considered the impact of asymptomatic COVID-19 cases on the disease's spread using an altered version of a SEIR dynamical model. Analytical and numerical estimation expressions of the basic reproduction number of COVID-19 in Saudi Arabia were obtained. He *et al.* [7] built an SEIR epidemic model for COVID-19 based on some universal methods of regulating. They used the Particle Swarm Optimization (PSO) algorithm to get an estimate of the system's parameters and employed the developed model to show the evolution of the pandemic. Dmitry *et al.* [8] used simple epidemic models to forecast the spread of COVID-19 in Russia and carried out a numerical forecast according to a public data set. They also presented a comparison between SIR and SEIR models. Their models predicted the highest number of contaminated people while sustaining quarantine measures. Cooper *et al.* [9] investigated the effectiveness of the spread of COVID-19 within some communities using an SIR model. They investigated the time evolution of various populations and monitored varied significant parameters for the spread of the disease. They concluded that the spread could be controlled if proper measures were adhered to. Munoz-Fernandez *et al.* [10] showed that the official data released by several authorities concerning COVID-19 were consistent with a non-autonomous SIR model. They constructed a model whose outcome fit available real data on COVID-19. They also predicted the development of the COVID-19 pandemic in some countries. Alenezi *et al.* [11] carried out an analysis of COVID-19 in Kuwait using an SIR model. They investigated the impact of preventive measures taken by Kuwait's local authorities to prevent the spread of COVID-19. Their investigation indicated the peak infection rate and anticipated dates for Kuwait. Liu [12] considered latent-infectious-recovery periods and carried out an analytical solution of an SIR-like model in Excel. He concluded that the simulated epidemic curve of the model fit perfectly with daily reported cases in the region mentioned in the paper. Zhu & Shen [13] proposed a modified SIR model to investigate the spread of COVID-19 for a specified period. Their investigation revealed that the cure rate was

approximately 0.05, while the reproduction number for the specified time was 0.4490.

Subrata *et al.* [14] proposed and analyzed an SEIR model. They studied the dynamical behavior and the stability of the model and compared the analysis of scenarios in two countries. Wintachai & Prathom [15] formulated an SEIR model that takes into account the efficiency of vaccination by forecasting the COVID-19 situation by the time vaccines were out.

Hospitalization, death, and testing data stability approximations were used by Albani *et al.* [25] to estimate underreported infections. Additionally, they evaluated how underreporting affected the development of vaccination plans. Daily COVID-19 reports from Chicago and New York City were used by Vinicius *et al.* [26] to estimate the parameters of an SEIR model that accounts for varying intensities. Impressively, their model was able to reproduce the observed data. Some other works also dealt with optimal control analysis, including [27-29].

In this paper, we offer a mathematical model of two COVID-19 strains. A mathematical analysis was carried out in conjunction with the epidemic indicator for the proposed models, the basic reproduction number for the model was derived, and finally the model's numerical simulation was analyzed. The rest of this paper is structured as follows. The mathematical formulation of the problem is offered in Section 2. The model analysis is presented in Section 3, including the positivity solution, the boundedness of the solution, the invariant region of the model, the basic reproduction number, and equilibria. Section 4 deals with the numerical simulation, and Section 5 contains the conclusion.

2 Model Problem

It is assumed in our models that once each strain is contracted, it gives persistent immunity to itself and other strains. We use a compartmental model with six compartments. These compartments are: Susceptible $S(t)$, Exposed $E(t)$, Infectious strain 1 $I_1(t)$, Infectious strain 2 $I_2(t)$, Quarantine $Q(t)$, Recovered $R(t)$. A susceptible individual, with a constant recruited rate Λ , can be infected by Strain 1 or by Strain 2 with transmission rate β_1 and β_2 respectively and move to the Exposed compartment. Individuals in the Exposed compartment show no symptoms and are unable to transmit the disease. After an incubation period of 5 to 14 days, individuals in the Exposed compartment become infectious at rate σ . A fraction λ of exposed individuals are fully infected by Strain 1, while the fraction of exposed individuals $(1 - \lambda)$ are fully infected by Strain 2 after the incubation period. The recovery rates for the two strains are γ_1 and γ_2 respectively, while α_1 and α_2 are the detection rates for Strains 1 and 2. θ is

the recovery rate from the Quarantine compartment. We assume natural mortality rate μ for individuals in all six compartments, while compartments $E(t), I_1(t), I_2(t)$ and $Q(t)$ have extra disease-induced death rate δ . The whole population $N(t)$ for the dynamic transmission at any time t is given by:

$$N(t) = S(t) + E(t) + I_1(t) + I_2(t) + Q(t) + R(t)$$

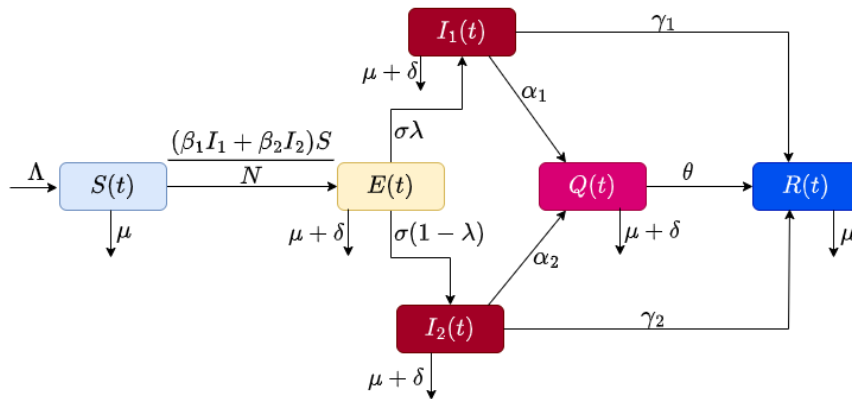


Figure 1 Compartmental diagram of disease transmission.

$$\left. \begin{aligned} \frac{dS(t)}{dt} &= \Lambda - \frac{\beta_1 I_1(t)S(t)}{N} - \frac{\beta_2 I_2(t)S(t)}{N} - \mu S(t) \\ \frac{dE(t)}{dt} &= \frac{\beta_1 I_1(t)S(t)}{N} + \frac{\beta_2 I_2(t)S(t)}{N} - (\sigma + \mu + \delta)E(t) \\ \frac{dI_1(t)}{dt} &= \lambda\sigma E(t) - (\gamma_1 + \alpha_1 + \mu + \delta)I_1(t) \\ \frac{dI_2(t)}{dt} &= (1 - \lambda)\sigma E(t) - (\gamma_2 + \alpha_2 + \mu + \delta)I_2(t) \\ \frac{dQ(t)}{dt} &= \alpha_1 I_1(t) + \alpha_2 I_2(t) - (\theta + \mu + \delta)Q(t) \\ \frac{dR(t)}{dt} &= \gamma_1 I_1(t) + \gamma_2 I_2(t) + \theta Q(t) - \mu R(t) \end{aligned} \right\} \quad (1)$$

with initial conditions

$$S(0) = S_0, E(0) = E_0, I_1(0) = I_{01}, I_2(0) = I_{02}, Q(0) = Q_0, R(0) = R_0.$$

The first four equations of (1) are independent of $R(t)$. We consider the sub-system and carry out an analysis on it.

$$\left. \begin{aligned} \frac{dS(t)}{dt} &= \Lambda - \frac{\beta_1 I_1(t)S(t)}{N} - \frac{\beta_2 I_2(t)S(t)}{N} - \mu S(t) \\ \frac{dE(t)}{dt} &= \frac{\beta_1 I_1(t)S(t)}{N} + \frac{\beta_2 I_2(t)S(t)}{N} - (\sigma + \mu + \delta)E(t) \\ \frac{dI_1(t)}{dt} &= \lambda \sigma E(t) - (\gamma_1 + \alpha_1 + \mu + \delta)I_1(t) \\ \frac{dI_2(t)}{dt} &= (1 - \lambda)\sigma E(t) - (\gamma_2 + \alpha_2 + \mu + \delta)I_2(t) \\ \frac{dQ(t)}{dt} &= \alpha_1 I_1(t) + \alpha_2 I_2(t) - (\theta + \mu + \delta)Q(t) \end{aligned} \right\} \quad (2)$$

with initial conditions

$$S(0) = S_0, E(0) = E_0, I_1(0) = I_{01}, I_2(0) = I_{02}, Q(0) = Q_0.$$

3 Model Analysis

In this section, we carry out a quantitative study of the two-strain model, including the positivity of the solution, the boundedness of the solution, the invariant region of the model, the basic reproduction number, equilibria, and the global stability of the model.

3.1 Positivity Solution

Theorem 1: The solutions $S(t), E(t), I_1(t), I_2(t), Q(t)$ of Equation (2) with positive initial condition are non-negative for all $t > 0$.

Proof: We will use the first equation in Equation (2) to show the positivity of the solutions.

Let

$$T = \text{Sup}\{t > 0 : S(t) > 0, E(t) > 0, I_1(t) > 0, I_2(t) > 0, Q(t) > 0\} \in [0, t].$$

For $t > 0$, then

$$\frac{dS(t)}{dt} = \Lambda - \left(\frac{\beta_1 I_1(t) + \beta_2 I_2(t)}{N} + \mu \right) S(t)$$

$$\frac{dS(t)}{dt} = \Lambda - (k(t) + \mu)S(t)$$

where $k(t) = \frac{\beta_1 I_1(t) + \beta_2 I_2(t)}{N}$

$$\frac{dS(t)}{dt} + (k(t) + \mu)S(t) = \Lambda$$

with integrating factor, we have:

$$\frac{d}{dt} \left(S(t) \exp \left\{ \mu t + \int_0^t k(p) dp \right\} \right) = \Lambda \exp \left\{ \mu t + \int_0^t k(p) dp \right\}$$

Solving and integrating both sides from 0 to T, we have:

$$S(T) = S(0) * \exp \left\{ - \left(\mu T + \int_0^T k(p) dp \right) \right\} + \exp \left\{ - \left(\mu t + \int_0^T k(p) dp \right) \right\} * \left[\int_0^T \Lambda * \exp \left\{ \mu t + \int_0^t k(p) dp \right\} dt \right] > 0. \quad (3)$$

From the result, we can see that $S(t)$ is strictly greater than zero. With the same argument, we can also prove that $E(t), I_1(t), I_2(t)$ and $Q(t)$ are all strictly greater than zero.

3.2 Boundedness of the Solution

Theorem 2: All solutions of Model (1) are bounded if $\lim_{t \rightarrow \infty} \text{Sup } N(t) \leq \frac{\Lambda}{\mu}$, then:

$$N(t) = E(t) + S(t) + Q(t) + R(t) + I_1(t) + I_2(t).$$

Proof: Let

$$0 < E(t) + Q(t) + R(t) + I_1(t) + I_2(t) \leq N(t) \quad (4)$$

Add up all the equations in Model (1), we have:

$$\frac{dN(t)}{dt} = \Lambda - \mu N(t) - \delta(E(t) + Q(t) + R(t) + I_1(t) + I_2(t)) \quad (5)$$

Using Eq. (4) in Eq. (5), we obtain:

$$\Lambda - \delta N(t) - \mu N(t) \leq \frac{dN(t)}{dt} \leq -\mu N(t) + \Lambda$$

It follows from this that the solutions of the proposed Model (1) are bounded and can be written as:

$$\frac{\Lambda}{\mu + \delta} \leq \lim_{t \rightarrow \infty} \text{Inf } N(t) \leq \lim_{t \rightarrow \infty} \text{Sup } N(t) \leq \frac{\Lambda}{\mu}. \quad (6)$$

3.3 Invariant Region of the Model

The parameters of the models are positive for all $t > 0$, for a biological region. The analysis of Model (1) will be in a meaningful biological region.

Lemma 1: The closed set Ω , defined by:

$\Omega = \left\{ (E(t) + S(t) + Q(t) + R(t) + I_1(t) + I_2(t)) \in \mathbb{R}_+^6 : N(t) \leq \frac{\Lambda}{\mu + \delta} \right\}$, is positive invariant for Model (1).

Proof: Let

$$\begin{aligned} N(t) &= E(t) + S(t) + Q(t) + R(t) + I_1(t) + I_2(t) \\ \frac{dN(t)}{dt} &= \frac{d}{dt} (E(t) + S(t) + Q(t) + R(t) + I_1(t) + I_2(t)) \\ \frac{dN(t)}{dt} &= \Lambda - \mu N(t) - \delta (E(t) + Q(t) + R(t) + I_1(t) + I_2(t)) \\ \frac{dN(t)}{dt} &= \Lambda - (\delta + \mu)N(t) \end{aligned}$$

After solving, we have:

$$\begin{aligned} N(t) &= \frac{\Lambda}{\delta + \mu} + N_0 e^{-(\delta + \mu)t}, \text{ where } N(0) = N_0 > 0 \\ \lim_{t \rightarrow \infty} N(t) &= \frac{\Lambda}{\delta + \mu} < N(t). \end{aligned}$$

Hence, we conclude that Ω is the positivity invariant for Model (1). Because of this, we can conclude that the solutions $(E(t), S(t), Q(t), R(t), I_1(t), I_2(t))$ tend to Ω .

3.4 The Basic Reproduction Number and its Associated Equilibria

3.4.1 The Basic Reproduction Number

Adopting the approach of Van den Driessche and Watmough [20-21], and utilizing the matrix of the next generation, we calculate the basic reproduction number in the following order. From the right-hand side of $E(t), I_1(t)$ and $I_2(t)$ of Model (1), there is an $\mathcal{F} - \mathcal{V}$ where \mathcal{F} represents the newly acquired infections in the population that is taken into consideration and \mathcal{V} corresponds to all the other terms in the compartments that are considered.

$$\begin{aligned} \mathcal{F} &= \begin{bmatrix} \frac{\beta_1 I_1(t)S(t) + \beta_2 I_2(t)S(t)}{N} \\ 0 \\ 0 \end{bmatrix}, \\ \mathcal{V} &= \begin{bmatrix} (\sigma + \mu + \delta)E(t) \\ -\lambda\sigma E(t) + (\gamma_1 + \alpha_1 + \mu + \delta)I_1(t) \\ -(1 - \lambda)\sigma E(t) + (\gamma_2 + \alpha_2 + \mu + \delta)I_2(t) \end{bmatrix} \end{aligned}$$

The Jacobian of \mathcal{F} and \mathcal{V} are evaluated and we obtain F and V as follows:

$$F = \begin{bmatrix} \frac{(\beta_1 I_1(t) + \beta_2 I_2(t))S(t)}{N^2} & \frac{\beta_1 S(t)}{N} & \frac{(\beta_1 I_1(t) + \beta_2 I_2(t))S(t)}{N^2} & \frac{\beta_2 S(t)}{N} & \frac{(\beta_1 I_1(t) + \beta_2 I_2(t))S(t)}{N^2} \\ 0 & 0 & 0 & 0 & 0 \\ 0 & 0 & 0 & 0 & 0 \end{bmatrix}$$

$$V = \begin{bmatrix} \sigma + \mu + \delta & 0 & 0 & 0 \\ -\lambda\sigma & \gamma_1 + \alpha_1 + \mu + \delta & 0 & 0 \\ -(1-\lambda)\sigma & 0 & \gamma_2 + \alpha_2 + \mu + \delta & 0 \end{bmatrix}$$

The Jacobian at the disease-free equilibrium, gives:

$$F = \begin{bmatrix} 0 & \beta_1 & \beta_2 \\ 0 & 0 & 0 \\ 0 & 0 & 0 \end{bmatrix}, V = \begin{bmatrix} \sigma + \mu + \delta & 0 & 0 \\ -\lambda\sigma & \gamma_1 + \alpha_1 + \mu + \delta & 0 \\ -(1-\lambda)\sigma & 0 & \gamma_2 + \alpha_2 + \mu + \delta \end{bmatrix}$$

$$V^{-1} = \begin{bmatrix} \frac{1}{\sigma + \delta + \mu} & 0 & 0 \\ \frac{\lambda\sigma}{(\sigma + \delta + \mu)(\gamma_1 + \alpha_1 + \mu + \delta)} & \frac{1}{\gamma_1 + \mu + \alpha_1 + \delta} & 0 \\ \frac{(1-\lambda)\sigma}{(\sigma + \delta + \mu)(\gamma_2 + \alpha_2 + \mu + \delta)} & 0 & \frac{1}{\gamma_2 + \alpha_2 + \mu + \delta} \end{bmatrix}$$

$$FV^{-1} = \begin{bmatrix} \frac{\beta_1 \lambda \sigma}{(\sigma + \delta + \mu)(\gamma_1 + \alpha_1 + \mu + \delta)} + \frac{\beta_2 (1-\lambda)\sigma}{(\sigma + \delta + \mu)(\gamma_2 + \alpha_2 + \mu + \delta)} & \frac{\beta_1}{\gamma_1 + \alpha_1 + \mu + \delta} & \frac{\beta_2}{\gamma_2 + \alpha_2 + \mu + \delta} \\ 0 & 0 & 0 \\ 0 & 0 & 0 \end{bmatrix}$$

The next-generation matrix of Equation (2) is FV^{-1} . The basic reproduction number R_0 of the combined strains is the spectral radius $\rho(FV^{-1})$, which is the non-negative matrix FV^{-1} .

$$R_0 = \rho(FV^{-1}) = \frac{\beta_1 \lambda \sigma}{(\sigma + \delta + \mu)(\gamma_1 + \alpha_1 + \mu + \delta)} + \frac{\beta_2 (1-\lambda)\sigma}{(\sigma + \delta + \mu)(\gamma_2 + \alpha_2 + \mu + \delta)}$$

$$R_0 = \rho(FV^{-1}) = R_0^1 + R_0^2$$

where,

$$R_0^1 = \frac{\beta_1 \lambda \sigma}{(\sigma + \delta + \mu)(\gamma_1 + \alpha_1 + \mu + \delta)} \text{ and } R_0^2 = \frac{\beta_2 (1-\lambda)\sigma}{(\sigma + \delta + \mu)(\gamma_2 + \alpha_2 + \mu + \delta)}$$

and the basic reproduction number is denoted by R_0^1 for Strain 1, and by R_0^2 for Strain 2.

3.4.2 Equilibrium State of the Proposed Model

The proposed Model (1) has two equilibrium states. The first one, the disease-free equilibrium, is the first, and the endemic equilibriums is the second. They are stated as follows:

1. $\xi_0 = \left(\frac{\Lambda}{\mu}, 0, 0, 0, 0, 0\right)$ is the disease-free equilibrium
2. Endemic equilibrium $\xi_1 = (S^*, E^*, I_1^*, I_2^*, Q^*, R^*)$, where

$$S^* = \frac{(\sigma + \delta + \mu)(\gamma_2 + \alpha_2 + \mu + \delta)(\gamma_1 + \alpha_1 + \mu + \delta)N}{\beta_2(1 - \lambda)\sigma(\gamma_1 + \alpha_1 + \mu + \delta) + \beta_1\lambda\sigma(\gamma_2 + \alpha_2 + \mu + \delta)} = \frac{\Lambda}{\mu R_0}$$

$$E^* = \frac{\Lambda\beta_1(R_0 - 1)((\sigma + \delta + \mu)(\gamma_2 + \alpha_2 + \mu + \delta)R_0 - \sigma\beta_2)}{(\sigma + \delta + \mu)^2(R_0)^2(\beta_1(\gamma_2 + \alpha_2) - \beta_2(\gamma_1 + \alpha_1) + (\beta_1 - \beta_2)\delta + (\beta_1 - \beta_2)\mu) + \frac{\Lambda\beta_2(R_0 - 1)\left(\frac{\sigma\beta_1}{R_0} - (\gamma_1 + \alpha_1 + \mu + \delta)(\sigma + \delta + \mu)\right)}{R_0(\sigma + \delta + \mu)^2((\delta + \mu)(\beta_1 - \beta_2) - \beta_2(\gamma_1 + \alpha_1) + \beta_1(\gamma_2 + \alpha_2))}}$$

$$I_1^* = \frac{\Lambda(R_0 - 1)((\sigma + \delta + \mu)(\gamma_2 + \alpha_2 + \mu + \delta)R_0 - \sigma\beta_2)}{(\sigma + \delta + \mu)R_0(\beta_1(\gamma_2 + \alpha_2) - \beta_2(\gamma_1 + \alpha_1) + (\beta_1 - \beta_2)\delta + (\beta_1 - \beta_2)\mu)}$$

$$I_2^* = \frac{\Lambda(R_0 - 1)\left(\frac{\sigma\beta_1}{R_0} - (\gamma_1 + \alpha_1 + \mu + \delta)(\sigma + \delta + \mu)\right)}{(\sigma + \delta + \mu)^2((\delta + \mu)(\beta_1 - \beta_2) - \beta_2(\gamma_1 + \alpha_1) + \beta_1(\gamma_2 + \alpha_2))}$$

$$Q^* = \frac{\Lambda\alpha_1(R_0 - 1)((\sigma + \delta + \mu)(\gamma_2 + \alpha_2 + \mu + \delta)R_0 - \sigma\beta_2)}{(\theta + \delta + \mu)(\sigma + \delta + \mu)R_0(\beta_1(\gamma_2 + \alpha_2) - \beta_2(\gamma_1 + \alpha_1) + (\beta_1 - \beta_2)\delta + (\beta_1 - \beta_2)\mu) + \frac{\Lambda\alpha_2(R_0 - 1)\left(\frac{\sigma\beta_1}{R_0} - (\gamma_1 + \alpha_1 + \mu + \delta)(\sigma + \delta + \mu)\right)}{(\sigma + \delta + \mu)((\delta + \mu)(\beta_1 - \beta_2) - \beta_2(\gamma_1 + \alpha_1) + \beta_1(\gamma_2 + \alpha_2))}}$$

$$R^* = \frac{\Lambda(R_0 - 1)A - B}{(\sigma + \delta + \mu)R_0(\beta_1(\gamma_2 + \alpha_2) - \beta_2(\gamma_1 + \alpha_1) + (\beta_1 - \beta_2)\delta + (\beta_1 - \beta_2)\mu)}$$

where

$$A = ((\gamma_2 - \gamma_1)\mu + (\gamma_1 - \gamma_2)\delta + (\gamma_1 - \gamma_2 + \alpha_1 - \alpha_2)\theta + \gamma_1\alpha_2 - \gamma_2\alpha_1)(\sigma + \delta + \mu)(\delta + \mu)R_0$$

and

$$B = ((\beta_2\gamma_1 - \beta_1\gamma_2)\mu + (\beta_2\gamma_1 - \beta_1\gamma_2)\delta + \theta(\alpha_1\beta_2 - \alpha_2\beta_1 - \beta_1\gamma_2 + \beta_2\gamma_1))\sigma$$

For the endemic equilibrium ξ_1 , we deduce that endemicity exist if $R_0 > 1$.

3.5 Local Stability

Theorem 3: The disease-free equilibrium point ξ_0 is locally asymptotically stable if $R_0 < 1$.

Proof: Examining the eigenvalues of the Jacobian matrix of Model (2) at

ξ_0 allows one to analyze the stability of the disease-free equilibrium. At equilibrium, the Jacobian matrix of Model (2) is given as:

$$J(\xi_0) = \begin{bmatrix} -\mu & 0 & -\beta_1 & \beta_2 & 0 \\ 0 & -(\sigma + \mu + \delta) & \beta_1 & \beta_2 & 0 \\ 0 & \lambda\sigma & -(\gamma_1 + \alpha_1 + \mu + \delta) & 0 & 0 \\ 0 & -(1-\lambda)\sigma & 0 & -(\gamma_2 + \alpha_2 + \mu + \delta) & 0 \\ 0 & 0 & \alpha_1 & \alpha_2 & -(\theta + \mu + \delta) \end{bmatrix}$$

The eigenvalues are:

$$\lambda_1 = -\mu, \lambda_2 = -(\theta + \mu + \delta), \lambda_3 = (\gamma_1 + \alpha_1 + \mu + \delta)(R_0^1 - 1),$$

$$\lambda_4 = \frac{(\gamma_1 + \alpha_1 + \mu + \delta)(R_0 - 1)}{R_0^1 - 1}, \lambda_5 = -\mu.$$

Since all the eigenvalues are negative, i.e., $\lambda_i = \text{negative}; i = 1..5$. Hence,

$R_0 < 1$, which means that the equilibrium without disease is asymptotically stable in the neighborhood.

3.6 Global Stability

Theorem 4: Point ξ_0 represents the disease-free equilibrium if $R_0^1 < 1$ and $R_0^2 < 1$ hold. This equilibrium is globally asymptotically stable.

Proof: By analogy with the non-linear Lyapunov function of the Goh-Volterra type used in [22-24], we consider the Lyapunov function in \mathbb{R}_+^4 , where S^q is defined at the disease-free equilibrium point ξ_0 , then:

$$L(S, E, I_1, I_2) = \left(S - S^q - S^q \ln\left(\frac{S}{S^q}\right) \right) + \frac{E}{\sigma + \mu + \delta} + \frac{I_1}{\lambda\sigma} + \frac{I_2}{(1-\lambda)\sigma}$$

Differentiated with respect to time t, we have:

$$L'(S, E, I_1, I_2) = \left(S' - S' \left(\frac{S}{S^q} \right) \right) + \frac{E'}{\sigma + \mu + \delta} + \frac{I_1'}{\lambda\sigma} + \frac{I_2'}{(1-\lambda)\sigma}$$

$$L'(S, E, I_1, I_2) = S' \left(1 - \left(\frac{S}{S^q} \right) \right) + \frac{E'}{\sigma + \mu + \delta} + \frac{I_1'}{\lambda\sigma} + \frac{I_2'}{(1-\lambda)\sigma}$$

$$\begin{aligned}
 &\leq \mu S^q \left(2 - \frac{S}{S^q} - \frac{S^q}{S} \right) + I_1 \left(\frac{\beta_1}{\sigma + \delta + \mu} - \frac{\gamma_1 + \alpha_1 + \mu + \delta}{\sigma \lambda} \right) \\
 &\quad + I_2 \left(\frac{\beta_2}{\sigma + \delta + \mu} - \frac{\gamma_2 + \alpha_2 + \mu + \delta}{\sigma(1 - \lambda)} \right) \\
 &\leq \mu S^q \left(2 - \frac{S}{S^q} - \frac{S^q}{S} \right) \\
 &\quad + I_1 \frac{\gamma_1 + \alpha_1 + \mu + \delta}{\sigma \lambda} \left(\frac{\beta_1 \sigma \lambda}{(\sigma + \delta + \mu)(\gamma_1 + \alpha_1 + \mu + \delta)} - 1 \right) \\
 &\quad + I_2 \frac{\gamma_2 + \alpha_2 + \mu + \delta}{\sigma(1 - \lambda)} \left(\frac{\beta_2 \sigma(1 - \lambda)}{(\sigma + \delta + \mu)(\gamma_2 + \alpha_2 + \mu + \delta)} - 1 \right) \\
 &\leq \mu S^q \left(2 - \frac{S}{S^q} - \frac{S^q}{S} \right) + I_1 \frac{\gamma_1 + \alpha_1 + \mu + \delta}{\sigma \lambda} (R_0^1 - 1) \\
 &\quad + I_2 \frac{\gamma_2 + \alpha_2 + \mu + \delta}{\sigma(1 - \lambda)} (R_0^2 - 1)
 \end{aligned}$$

Let $y = \frac{S^q}{S}$,

$$\therefore \frac{S}{S^q} = \frac{1}{y}, \text{ then } 2 - \frac{S}{S^q} - \frac{S^q}{S} \Rightarrow 2 - \frac{1}{y} - y = \frac{-(y - 1)^2}{y} \leq 0$$

This implies that the disease-free equilibrium ξ_0 is globally asymptotic stable if and only if $R_0^1 < 0$ and $R_0^2 < 0$. Then, we have:

$$L'(S, E, I_1, I_2) \leq 0.$$

3.7 Sensitivity Analysis

To establish the robustness of the model prediction to the parameter values, a sensitivity analysis is commonly used. As a result of this, studying the sensitivity is very important in a dynamic system. Here we estimate the sensitivity indices for basic reproduction number R_0 .

Proposition 1: With β_1 and β_2 , the basic reproduction number increases.

Proof: This follows from the fact that when the basic reproduction number is varied, we have the following:

$$\begin{aligned}
 \frac{\partial R_0}{\partial \beta_1} &= \frac{\sigma \lambda}{(\sigma + \delta + \mu)(\lambda_1 + \mu + \alpha_1 + \delta)} > 0, \\
 \frac{\partial R_0}{\partial \beta_2} &= \frac{\sigma(1 - \lambda)}{(\sigma + \delta + \mu)(\lambda_2 + \mu + \alpha_2 + \delta)} > 0.
 \end{aligned}$$

for any parameter values and $0 \leq \lambda < 1$.

Proposition 2: The basic reproduction number decreases with $\delta, \gamma_1, \gamma_2, \alpha_1, \alpha_2, \mu$ and λ .

Proof: This follows from the fact that when the basic reproduction number is varied, we have the following:

$$\frac{\partial R_0}{\partial \gamma_1} < 0, \frac{\partial R_0}{\partial \gamma_2} < 0, \frac{\partial R_0}{\partial \alpha_1} < 0, \frac{\partial R_0}{\partial \alpha_2} < 0,$$

$$\frac{\partial R_0}{\partial \delta} < 0, \frac{\partial R_0}{\partial \mu} < 0 \text{ and } \frac{\partial R_0}{\partial \lambda} < 0$$

for any parameter values and $0 \leq \lambda < 1$.

Definition 1: [18-19] The normalized forward sensitivity index of a variable \mathbb{H} that depends differentially on a parameter ζ is defined as:

$$\mathcal{V}_{\zeta}^{\mathbb{H}} = \frac{\partial \mathbb{H}}{\partial \zeta} \times \frac{\zeta}{|\mathbb{H}|}$$

The largest possible value for $\mathcal{V}_{\zeta}^{\mathbb{H}}$ is 1. If the magnitude is 1, then an increase of $y\%$ in ζ would result in an increase of $y\%$ in \mathbb{H} . For the same reason, if you reduce ζ by $y\%$, \mathbb{H} will also go down by $y\%$. However, $\mathcal{V}_{\zeta}^{\mathbb{H}}$ must be at least -1. Therefore, if ζ is increased by $y\%$, \mathbb{H} is decreased by $y\%$, and if ζ is decreased by $y\%$, \mathbb{H} is increased by $y\%$.

The following table displays the model’s parameter baseline evaluation of the R_0 sensitivity indices.

Table 1 Sensitivity index.

S/n	Parameter	Sensitivity index	Comment
1.	β_1	+0.44	Enhanced disease spread
2.	β_2	+0.56	Enhanced disease spread
3.	σ	+0.046	Enhanced disease spread
4.	μ	-0.00011	Eradicate disease
5.	δ	-0.069	Eradicate disease
6.	γ_1	-0.356	Eradicate disease
7.	γ_2	-0.454	Eradicate disease
8.	α_1	-0.073	Eradicate disease
9.	α_2	-0.094	Eradicate disease
10.	λ	-0.120	Eradicate disease

From the above table, the most sensitive parameter is β_2 . Since $\mathcal{V}_{\zeta}^{\mathbb{H}} = 0.56$, if β_2 is decreased (or increases) by 10%, then R_0 will be decreased (or increased) by 5.6%.

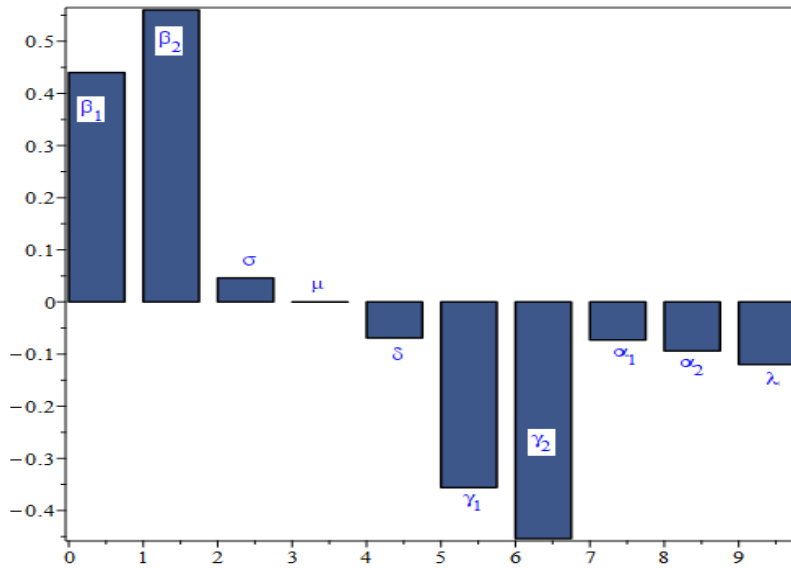


Figure 2 Sensitivity indices for parameters in R_0 .

The normalized forward sensitivity indices of the basic reproduction number with respect to each of the baseline parameter values is displayed in Figure 2.

3.8 Bifurcation analysis

In this section, we adopt Castillo-Chavez & Song [16] to analyze the bifurcation analysis of Model (2.2). Introducing

$$s = \frac{S(t)}{N} = x_1, e = \frac{E(t)}{N} = x_2, i_1 = \frac{I_1(t)}{N} = x_3, i_2 = \frac{I_2(t)}{N} = x_4,$$

$q = \frac{Q(t)}{N} = x_5$, the system (2) becomes:

$$\begin{aligned} \frac{dx_1}{dt} &= \Lambda - \beta_1 x_1 x_3 - \beta_2 x_1 x_4 - \mu x_1 := f_1 \\ \frac{dx_2}{dt} &= \beta_1 x_1 x_3 + \beta_2 x_1 x_4 - (\sigma + \mu + \delta) x_2 := f_2 \\ \frac{dx_3}{dt} &= \lambda \sigma x_2 - (\gamma_1 + \alpha_1 + \mu + \delta) x_3 := f_3 \\ \frac{dx_4}{dt} &= (1 - \lambda) \sigma x_2 - (\gamma_2 + \alpha_2 + \mu + \delta) x_4 := f_4 \end{aligned} \tag{7}$$

We assume that the bifurcation parameter is λ . The condition that $R_0 = 1$ implies

$$\lambda = \frac{(\delta^2 + 2\delta\mu + \delta\sigma + \delta\alpha_2 + \delta\gamma_2 + \mu^2 + \sigma\mu + \mu\alpha_2 + \mu\gamma_2 + \sigma\alpha_2 - \sigma\beta_2 + \sigma\gamma_2)(\gamma_1 + \alpha_1 + \mu + \delta)}{\sigma(\delta\beta_1 - \delta\beta_2 + \mu\beta_1 - \mu\beta_2 - \alpha_1\beta_2 + \alpha_2\beta_1 + \gamma_2\beta_1 - \gamma_1\beta_2)} := \lambda^*$$

Describing the general system of ODEs such that

$$\frac{dx}{dt} = f(x, \lambda^*), f: \mathbb{R}^n \times \mathbb{R}^n, f \in C^2(\mathbb{R}^n \times \mathbb{R}^n)$$

For the above-described system and for all values of the parameters ϕ , it is assumed that zero represents a state of equilibrium, i.e., $f(0, \lambda^*) \equiv 0, \forall \lambda^* = 0$.

The eigenvalues of the matrix, $J(\xi_0, \lambda^*)$ are given as:

$$s_1 = -\mu, s_2 = -(\theta + \mu + \delta), s_3 = -(\gamma_1 + \alpha_1 + \alpha_2 + 2\mu + 2\delta), s_0 = 0.$$

The right eigenvector of the matrix $J(\xi_0, \lambda^*)$ at zero eigenvalues is:

$$\begin{bmatrix} -\mu & 0 & -\beta_1 & -\beta_2 \\ 0 & -(\sigma + \mu + \delta) & \beta_1 & \beta_2 \\ 0 & \lambda^* \sigma & -(\gamma_1 + \alpha_1 + \mu + \delta) & 0 \\ 0 & \sigma(1 - \lambda^*) & 0 & -(\gamma_2 + \alpha_2 + \mu + \delta) \end{bmatrix} \begin{bmatrix} w_1 \\ w_2 \\ w_3 \\ w_4 \end{bmatrix} = \begin{bmatrix} 0 \\ 0 \\ 0 \\ 0 \end{bmatrix}$$

This implies:

$$\begin{aligned} -\mu w_1 - \beta_1 w_3 - \beta_2 w_4 &= 0 \\ -(\sigma + \mu + \delta) w_2 + \beta_1 w_3 + \beta_2 w_4 &= 0 \\ \sigma \lambda^* w_2 - (\alpha_1 + \gamma_1 + \mu + \delta) w_3 &= 0 \\ \sigma(1 - \lambda^*) w_2 - (\alpha_2 + \gamma_2 + \mu + \delta) w_4 &= 0 \end{aligned}$$

After solving, we have:

$$\begin{aligned} w_1 &= -\left(\frac{\beta_1 \sigma \lambda^*}{\mu} + \frac{\beta_2 (\alpha_2 + \gamma_2 + \mu + \delta)}{\mu \sigma (1 - \lambda^*) (\alpha_1 + \gamma_1 + \mu + \delta)} \right), \\ w_2 &= \alpha_2 + \gamma_1 + \mu + \delta, w_3 = \sigma \lambda^* \\ w_4 &= \frac{\alpha_2 + \gamma_2 + \mu + \delta}{\sigma (1 - \lambda^*) (\alpha_1 + \gamma_1 + \mu + \delta)}. \end{aligned}$$

The right eigenvector is:

$$w = \begin{bmatrix} -\left(\frac{\beta_1 \sigma \lambda^*}{\mu} + \frac{\beta_2 (\alpha_2 + \gamma_2 + \mu + \delta)}{\mu \sigma (1 - \lambda^*) (\alpha_1 + \gamma_1 + \mu + \delta)} \right) \\ \alpha_2 + \gamma_1 + \mu + \delta \\ \sigma \lambda^* \\ \frac{\alpha_2 + \gamma_2 + \mu + \delta}{\sigma (1 - \lambda^*) (\alpha_1 + \gamma_1 + \mu + \delta)} \end{bmatrix} \quad (8)$$

Moreover, the left eigenvector $\mathbf{v} = (v_1, v_2, v_3, v_4)$, accomplishing $\mathbf{v} * \mathbf{w} = 1$, is given as:

$$\begin{aligned} -\mu v_1 &= 0 \\ -(\sigma + \mu + \delta)v_2 + \sigma\lambda^* v_3 + \sigma(1 - \lambda^*)v_4 &= 0 \\ -\beta_1 v_1 + \beta_1 v_2 - (\alpha_1 + \gamma_1 + \mu + \delta)v_3 &= 0 \\ -\beta_2 v_1 + \beta_2 v_2 - (\alpha_2 + \gamma_2 + \mu + \delta)v_4 &= 0 \end{aligned}$$

Then the left eigenvector is therefore:

$$\begin{aligned} v_1 &= 0, v_2 = \frac{1}{\alpha_1 + \gamma_1 + \mu + \delta} - \frac{\alpha_2 + \gamma_2 + \mu + \delta}{\alpha_1 + \gamma_1 + \mu + \delta} \left[\beta_1 \sigma \lambda^* - \frac{\beta_2}{\sigma(1 - \lambda^*)} \right], \\ v_3 &= \beta_1(\alpha_2 + \gamma_2 + \mu + \delta), v_4 = \beta_2(\alpha_1 + \gamma_2 + \mu + \delta) \end{aligned}$$

i.e.,

$$\mathbf{v} = \left(0, \frac{1}{\alpha_1 + \gamma_1 + \mu + \delta} - \frac{\alpha_2 + \gamma_2 + \mu + \delta}{\alpha_1 + \gamma_1 + \mu + \delta} \left[\beta_1 \sigma \lambda^* - \frac{\beta_2}{\sigma(1 - \lambda^*)} \right], \beta_1(\alpha_2 + \gamma_2 + \mu + \delta), \beta_2(\alpha_1 + \gamma_2 + \mu + \delta) \right) \tag{9}$$

In a disease-free equilibrium, we estimate the partial derivatives and obtain:

$$\begin{aligned} \frac{\partial^2 f_1}{\partial x_1 \partial x_3} = \frac{\partial^2 f_1}{\partial x_3 \partial x_1} = -\beta_1, \frac{\partial^2 f_1}{\partial x_1 \partial x_4} = \frac{\partial^2 f_1}{\partial x_4 \partial x_1} = -\beta_2, \\ \frac{\partial^2 f_2}{\partial x_1 \partial x_3} = \frac{\partial^2 f_2}{\partial x_3 \partial x_1} = \beta_1, \frac{\partial^2 f_2}{\partial x_1 \partial x_4} = \frac{\partial^2 f_2}{\partial x_4 \partial x_1} = \beta_2, \\ \frac{\partial^2 f_3}{\partial x_2 \partial \lambda} = \sigma, \frac{\partial^2 f_4}{\partial x_2 \partial \lambda} = -\sigma, \end{aligned}$$

while the remaining second-order derivatives go to zero.

Coefficients \mathbf{a} and \mathbf{b} are calculated using the definition given by Castillo-Chavez and Song [16], i.e., assuming that f_k is the k-th component of f and

$$\begin{aligned} \mathbf{a} &= \sum_{k,i,j=1}^4 v_k w_i w_j \frac{\partial^2 f_k}{\partial x_i \partial x_j} (\xi_0, \lambda^*) \\ \mathbf{b} &= \sum_{k,i,j=1}^4 v_k w_i \frac{\partial^2 f_k}{\partial x_i \partial \lambda} (\xi_0, \lambda^*) \end{aligned}$$

The local dynamics of Model 2 are entirely estimated by the coefficients \mathbf{a} and \mathbf{b} around $x = 0$. Taking into consideration the system of equations (7) and

estimating the coefficients \mathbf{a} and \mathbf{b} , all derivative terms other than zero for $\frac{\partial^2 f_k}{\partial x_i \partial x_j}(\xi_0, \lambda^*)$ and $\frac{\partial^2 f_k}{\partial x_i \partial \lambda}(\xi_0, \lambda^*)$ are as follows:

$$\mathbf{a} = 2v_1 w_1 w_3 \frac{\partial^2 f_1}{\partial x_1 \partial x_3}(\xi_0, \lambda^*) + 2v_1 w_1 w_4 \frac{\partial^2 f_1}{\partial x_1 \partial x_4}(\xi_0, \lambda^*) + 2v_2 w_1 w_3 \frac{\partial^2 f_2}{\partial x_1 \partial x_3}(\xi_0, \lambda^*) + 2v_2 w_1 w_4 \frac{\partial^2 f_2}{\partial x_1 \partial x_4}(\xi_0, \lambda^*)$$

and

$$\mathbf{b} = v_4 w_2 \frac{\partial^2 f_4}{\partial x_1 \partial \lambda}(\xi_0, \lambda^*)$$

Using Equations (8) and (9) with some partial second-order derivatives obtained from System (7), we get:

$$a = \frac{2(\lambda^* \sigma^2 \beta_1 (\lambda^* - 1) + \beta_2) MN}{3\sigma \mu (\lambda^* - 1)^3 (\gamma_1 + \alpha_1 + \mu + \delta)^2} > 0$$

where

$$M = ((\lambda^* - 1)\{\lambda^* \sigma^2 \beta_1 (\gamma_2 + \alpha_2 + \mu + \delta) + \sigma\} + \beta_2 (\gamma_2 + \alpha_2 + \mu + \delta))$$

and

$$N = ((\lambda^* - 1)\lambda^* \sigma^2 \beta_1 (\gamma_1 + \alpha_1 + \mu + \delta) - (\gamma_2 + \alpha_2 + \mu + \delta))$$

Also,

$$\mathbf{b} = -\sigma \beta_2 (\gamma_1 + \alpha_1 + \mu + \delta)^2 < 0.$$

It can be seen that \mathbf{a} is a positive coefficient, while \mathbf{b} is a negative coefficient. According to Castillo-Chevez & Song [16], if $a > 0, b < 0$ when $\lambda^* < 0$, the system is unable to maintain its stability and there exists a negative and locally asymptotically stable negative equilibrium.

Define:

$$R_0^{**} = \frac{\beta_1 \lambda^* \sigma}{(\sigma + \mu + \delta)(\gamma_1 + \alpha_1 + \mu + \delta)} + \frac{\beta_1 (1 - \lambda^*) \sigma}{(\sigma + \mu + \delta)(\gamma_2 + \alpha_2 + \mu + \delta)}.$$

If $R_0^{**} < 1$, then $a < 0$ and if $R_0^{**} > 1$, then $a > 0$. Therefore, the following follows: if $R_0^{**} > 1$, the first four equations in System (2) exhibit backward bifurcation when $R_0 = 1$. If $R_0^{**} < 1$, the first four equations in System (2) exhibit forward bifurcation when $R_0 = 1$.

4 Numerical Simulation

We devote this section to performing a numerical simulation of the formulated two-strain Covid-19 model. The model is solved numerically in R using the deSolve package. The estimated and fitted parameters utilized in the simulation process are given in Table 1. Susceptible, Exposed, Infected by Strain 1, Infected by Strain 2, Quarantine and Recovery at initial time $t = 0$ are given respectively as: $S(0) = 3978, E(0) = 7000, I_1(0) = 4000, I_2(0) = 2500, Q(0) = 4000$ and $R(0) = 0$. We assume there are no recovered individuals at the initial level.

Table 2 Parameter values for the Covid-19 model.

Parameter	Description	Value	Source
μ	Natural death rate	0.000422536	Estimated
λ	Fraction of individuals infected by Strain 1	0.5	Estimated
β_1	Transmission rate to Strain 1	$\frac{1}{14}$	Estimated
β_2	Transmission rate to Strain 2	$\frac{1}{11}$	Estimated
δ	Death rate due to Strain 1 or 2	0.0276	Estimated
σ	Progression rate to the Infectious compartment from the Exposed compartment	$\frac{1}{7}$	Estimated
γ_1, γ_2	Recovery rates from the Infectious compartment	0.97	Estimated
α_1, α_2	Detention rates from the Infectious compartment to the Quarantine compartment	0.2	[17]
θ	Recovery rate from the Quarantine compartment	$\frac{1}{12}$	Estimated

The results obtained from the numerical simulation are depicted in the figures below. Figure 3 presents an overview of what happens in the five compartments. The figure shows that more people recovered from the two strains and the epidemic curve flattened after some time. The number of quarantine compartments increased from the starting day and reached its peak at the end of the fifth day. After the fifth day, the number of individuals in the Quarantine compartment decreased. It can also be seen that the Strain 1 and Strain 2 compartments decreased until day 20, when the number of people in that compartment was reduced to zero. The number of people who were exposed to the disease also declined, as can be seen in the figure, whereby we experience more recovery. The number of susceptible individuals slightly decreased at the start and remained steady throughout.

Figure 4 shows that the number of individuals in the Infected compartments of Strain 1 and Strain 2 rose for a period before they started declining, while the Exposed compartment decreased.

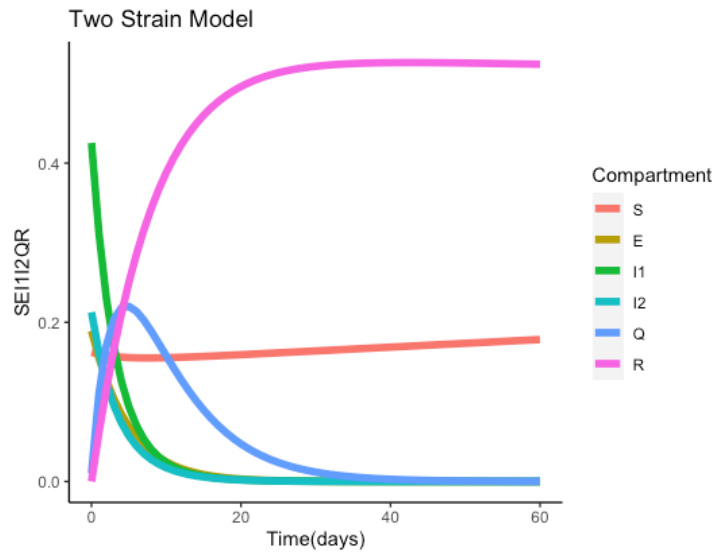


Figure 3 Dynamic of the six compartments.

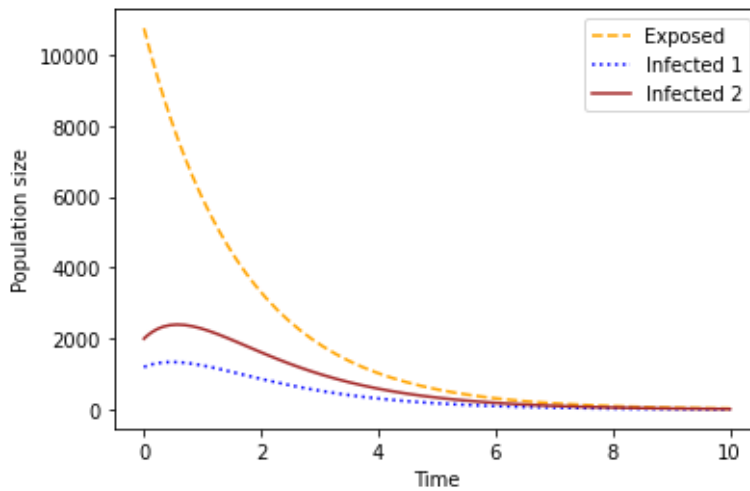


Figure 4 Behavior of Exposed, Strain 1 and Strain 2.

Figures 5-7 shows the impacts of increasing σ , β_1 and β_2 on recovery. It can be seen in Figure 5 that as the progression rate increased there existed an increase in the Recovery compartment at all times. This implies that more people recovered when they contracted the disease. The impact of the transmission rate of Strain 2 is investigated in Figure 6. We notice that at first there is no difference, but as time goes on, an increase in the transmission rate of Strain 2 appears. We notice

that more people recovered. The same also applied to Strain 1, as shown in Figure 7.

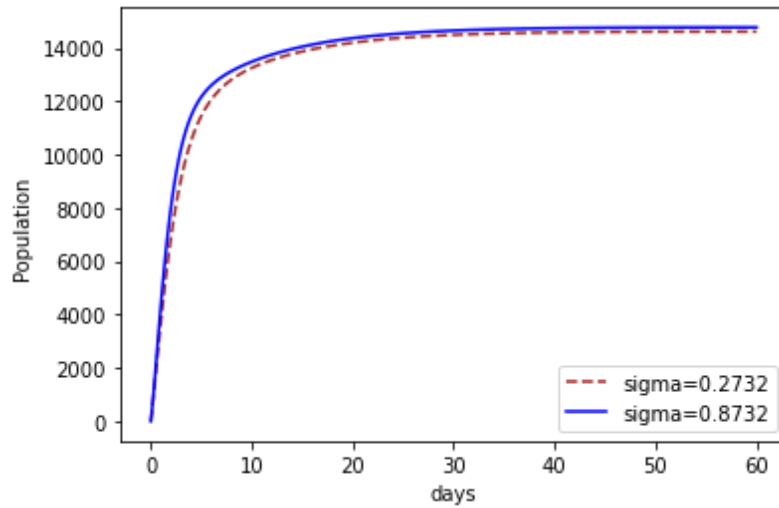


Figure 5 The effect of increasing σ on recovery.

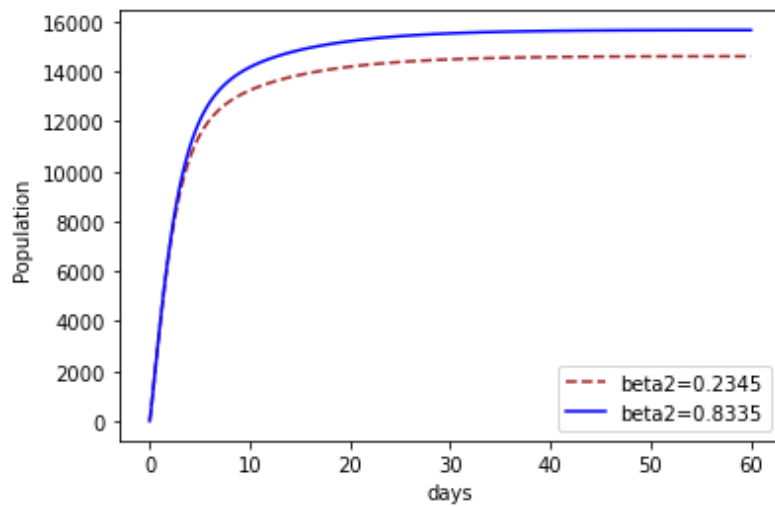


Figure 6 The effect of increasing β_2 on recovery.

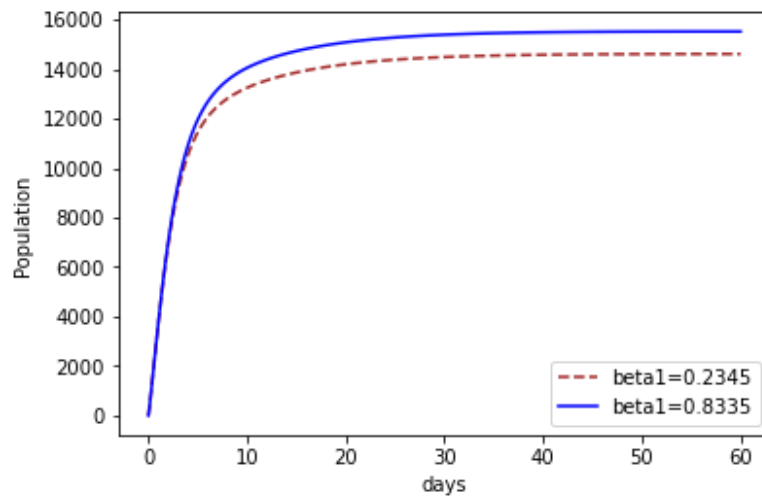


Figure 7 The effect of increasing β_1 on recovery.

5 Conclusions

We considered a system of mathematical equations that reports the dynamics of two COVID-19 strains without control or treatment. The analysis of the system was well established. We presented a stability analysis of the disease-free equilibrium and the endemic equilibrium based on the estimated basic reproduction number. Whenever $R_0 < 1$, the disease-free equilibrium is locally asymptotically stable and it is globally asymptotic stable if and only if $L'(S, E, I_1, I_1) < 0$. We presented a bifurcation analysis for the formulated problem and concluded that if $R_0^{**} > 1$, the first four equations in System (2) exhibit backward bifurcation when $R_0 = 1$. If $R_0^{**} < 1$, the first four equations in System (2) exhibit forward bifurcation when $R_0 = 1$. We also presented a numerical simulation to see the dynamics of the six compartments and the impact of some parameters on recovery.

References

- [1] WHO, *Coronavirus Disease 2019 (Covid-19) Situation Report-62*, March 2020.
- [2] <https://www.who.int/emergencies/diseases/novel-coronavirus-2019/question-and-answers-hub/q-a-detail/coronavirus-disease-covid-19-how-is-it-transmitted>
- [3] Wickramaarachchi, W.P.T.M., Perera, S.S.N. & Jayasinghe, S., *COVID-19 Epidemic in Sri Lanka: A Mathematical and Computational Modelling*

- Approach to Control. Computational and Mathematical Methods in Medicine*, Article ID 4045064, **9**(2020), 2020.
- [4] Mohsen, A. A., Al-Husseiny, H. F., Zhou, X. & Hattaf, K., *Global Stability of COVID-19 Model Involving the Quarantine Strategy and Media Coverage Effect*, AIMS Public Health, **7**(3), pp. 587-605, 2020.
- [5] Seidu, B., *Optimal Strategies for Control of COVID-19: A Mathematical Perspective*, Scientifica, **2020**(12), Article ID 4676274, 2020.
- [6] Alshammari, F.S., *A Mathematical Model to Investigate the Transmission of COVID-19 in the Kingdom of Saudi Arabia. Computational and Mathematical Methods in Medicine*, Article ID 9136157, **2020**(13), 2020.
- [7] Shaobo, H., Yuexi, P. & Kehui, S., *SEIR Modelling of The COVID-19 and Its Dynamics*, Nonlinear Dynamics, **101**, pp. 1667-1680, 2020.
- [8] Dmitry, A., Tomchin, D.A. & Fradkov, A.L., *Prediction of The COVID-19 Spread in Russia Based on SIR and SEIR Models of Epidemic*, IFAC Papers online, **53**(5), pp. 833-838, 2020.
- [9] Cooper, I., Argha Mondal, A. & Antonopoulos, C.G., *A SIR Model Assumption for The Spread of COVID-19 in Different Communities*, Chaos, Solitons and Fractals, **139**, pp. 110057, 2020.
- [10] Muñoz-Fernández, G.A., Seoane, J.M. & Seoane-Sepúlveda, J.B., *A SIR-Type Model Describing the Successive Waves of COVID-19*, Chaos, Solitons and Fractals, **144**, pp. 110682, 2021.
- [11] Alenezi, M.N., Al-Anzi, F.S. & Alabdulrazzaq, H., *Building a Sensible SIR Estimation Model for COVID-19 Outspread in Kuwait*. Alexandria Engineering Journal, **60**, pp. 3161-3175, 2021.
- [12] Liu, X., *A Simple, SIR-Like but Individual-Based Epidemic Model: Application in Comparison of COVID-19 In New York City and Wuhan*, Results in Physics, **20**, pp. 103712, 2021.
- [13] Zhu, W.J. & Shen, S.F., *An Improved SIR Model Describing the Epidemic Dynamics of The COVID-19 In China*. Results in Physics, **25**, pp. 104289, 2021.
- [14] Subrata, P.A., Animesh, M.B., Uttam, G.C. & Banamali, R. D., *Study of SEIR Epidemic Model and Scenario Analysis of Covid-19 Pandemic*, Ecological Genetics and Genomics, **19**, pp. 100087, 2021.
- [15] Phitchayapak W. & Kiattisak P., *Stability Analysis of SEIR Model Related to The Efficiency of Vaccines for COVID-19 Situation*, Heliyon, **7**, pp. e06812, 2021.
- [16] Castillo-Chavez, C. & Song, B., *Dynamical Models of Tuberculosis and Their Applications*, Math Biosci. Eng., **1**, pp. 361-404, 2004.
- [17] Tang, B., Xia, F., Tang, S., Bragazzi, N.L., Li, Q., Sun, X., Liang, J., Xia, Y. & Wu, J., *The Effectiveness of Quarantine and Isolation Determine the Trend of The COVID-19 Epidemics in The Final Phase of the Current Outbreak in China*, International Journal of Infectious Diseases, **95**, pp. 288-293, 2020.

- [18] Chitnis, N., Hyman, J.M. & Cushing, J.M., *Determining Important Parameters in the Spread of Malaria Through the Sensitivity Analysis of a Mathematical Model*, Bulletin of Mathematical Biology, **70**, pp. 1272-1296, 2008. DOI 10.1007/s11538-008-9299-0.
- [19] Berhe, H.W., Makinde, O.D. & Theuri, D.M., *Parameter Estimation and Sensitivity Analysis of Dysentery Diarrhoea Epidemic Mode*, J. Appl. Math., **1**(13), 2019.
- [20] Driessche, P.V. & Watmough, J., *Reproduction Numbers and Sub-Threshold Endemic Equilibria for Compartmental Models of Disease Transmission*, Mathematical Biosciences, **180**, pp. 29-48, 2002.
- [21] Diekmann, O., Heesterbeek, J. A. P. & Roberts, M. G., *The Construction of Next Generation Matrices for Compartmental Epidemic Models*, Journal of the royal society interface, **7**(47), pp. 873-885, 2010.
- [22] Beretta, E. & Takeuchi, Y., *Global Stability of Lotka-Volterra Diffusion Models with Continuous Time Delay*, SIAM J. Appl. Math., **48**(3), pp. 627-651, 1988.
- [23] Goh, B. S., *Global Stability in Two Species Interactions*, J. Math. Biol., **3**, pp. 313-318, 1976.
- [24] Korobeinikov, A., *Global Properties of SIR and SEIR Epidemic Models with Multiple Parallel Infectious Stages*, Bull. Math. Biol., **71**(1), pp. 1-13, 2021.
- [25] Albani, V., Loria, J., Massad, E. & Zubelli, J., *COVID-19 Underreporting and Its Impact on Vaccination Strategies*. BMC Infectious Diseases, **21**(1), pp. 75-83, 2009.
- [26] Albani, V., Loria, J., Massad, E. & Zubelli, J., *The Impact of Covid-19 Vaccination Delay: Adata-Driven Modelling Analysis for Chicago and New York City*, Vaccine, **39**(41), pp. 76088-6094, 2009.
- [27] Tilahun, G.T., Makinde, O.D. & Malonza, D., *Co-Dynamics of Pneumonia and Typhoid Fever Diseases with Cost-Effective Optimal Control Analysis*, Applied Mathematics and computation, **316**, pp. 438-459, 2018.
- [28] Berhe, H.W., Makinde, O.D. & Theuri, D.M., *Co-Dynamics of Measles and Dysentery Diarrhea Diseases with Optimal Control and Cost-Effectiveness Analysis*, Applied Mathematics and Computation, **347**, pp. 903-921, 2019.
- [29] Keno, T.D., Makinde, O.D. & Obsu, L.L., *Optimal Control and Cost Effectiveness Analysis of SIRS Malaria Disease Model with Temperature Variability Factor*, Journal of Mathematical & Fundamental Sciences, **53**(1), pp. 134-163, 2021.